Production d'énergie (hydraulique, thermique et nucléaire)

CALCUL DES FORCES FLUIDELASTIQUES DANS LES FAISCEAUX DE TUBES SOUS ECOULEMENT AXIAL : THEORIE, VALIDATION, APPLICATION AUX ASSEMBLAGES COMBUSTIBLES DES REP

AN ANALYTICAL MODEL FOR THE PREDICTION OF FLUIDELASTIC FORCES IN A ROD BUNDLE SUBJECTED TO AXIAL FLOW : THEORY, EXPERIMENTAL VALIDATION AND APPLICATION TO PWR FUEL ASSEMBLIES

97NB00079

L

DIRECTION DES ÉTUDES ET RECHERCHES

SERVICE RÉACTEURS NUCLÉAIRES ET ECHANGEURS
DÉPARTEMENT TRANSFERTS THERMIQUES ET AÉRODYNAMIQUE

EDF
Electricité de France

Juin 1997

BEAUD F.

CALCUL DES FORCES FLUIDELASTIQUES DANS LES FAISCEAUX DE TUBES SOUS ECOULEMENT AXIAL : THEORIE, VALIDATION, APPLICATION AUX ASSEMBLAGES COMBUSTIBLES DES REP

AN ANALYTICAL MODEL FOR THE PREDICTION OF FLUIDELASTIC FORCES IN A ROD BUNDLE SUBJECTED TO AXIAL FLOW : THEORY, EXPERIMENTAL VALIDATION AND APPLICATION TO PWR FUEL ASSEMBLIES

Pages : 15

97NB00079

Diffusion : J.-M. Lecœuvre
EDF-DER
Service IPN. Département PROVAL
1, avenue du Général-de-Gaulle
92141 Clamart Cedex

ISSN 1161-0611

SYNTHÈSE :

Les assemblages combustibles des cœurs REP sont soumis à l'écoulement axial du fluide primaire. La turbulence de l'écoulement est une source de vibration des crayons combustibles, au même titre que toute excitation mécanique externe. Les champs moyens de pression et de vitesse dépendent du mouvement des crayons combustibles. Par conséquent, les variations de forces de pression et de forces visqueuses sont fonction du mouvement des structures. Dans le cas des écoulements axiaux, il est connu que le couplage fluide-structure provenant de ces forces, dites fluidélastiques, engendre une importante augmentation de l'amortissement du système mécanique sous sollicitation fluide. Il est donc primordial de tenir compte de ces forces fluidélastiques dans l'étude d'un tel système dynamique.

Cette note présente un modèle analytique calculant les forces fluidélastiques dans des faisceaux de cylindres circulaires élancés et soumis à un écoulement axial turbulent de fluide dense. Ce modèle, développé sur la base d'idées proposées par Païdoussis et Chen, utilise une méthode de perturbation et se place dans le cadre de l'hypothèse quasi-stationnaire pour évaluer les forces fluides visqueuses, en supposant notamment que les couches limites sont très minces et restent attachées aux cylindres. Le calcul des forces fluidélastiques visqueuses revient à considérer l'effet d'un écoulement oblique autour d'un cylindre incliné avec une très faible incidence : un seul paramètre physique, correspondant à la valeur de la dérivée du coefficient de portance à angle d'incidence nul, fait l'objet d'une loi de fermeture. Cette unique paramètre est estimé par comparaison des prédictions du modèle avec les résultats expérimentaux de Tanaka & Hotta. Dans cette note, les hypothèses du modèle sont toutes clairement justifiées. Une approche originale est proposée pour pouvoir prendre en compte dans le modèle analytique une enceinte rectangulaire canalisant l'écoulement. Elle est sur une extension de la méthode dite des "images".

Afin d'approfondir l'étude des phénomènes d'interaction fluide-structure dans les faisceaux de tubes sous écoulement axial, une maquette a été mise au point à la DER. Elle se compose de 9 tubes Inox, souples ou rigides, disposés en faisceau à pas carré à l'intérieur d'une enceinte de confinement carrée. Elle a été dimensionnée en similitude vibratoire avec un faisceau 3 x 3 de crayons combustibles (même pas réduit, mêmes gammes de fréquences réduites et de Reynolds) de façon à pouvoir valider le modèle dans des conditions aussi proches que possible que celles des assemblages combustibles pour lesquelles il a été initialement prévu. Les valeurs des caractéristiques vibratoires (fréquences, amortissements réduits, ...) sont déduites des signaux issus de jauges de contrainte post-traités à l'aide d'un logiciel d'identification modale dans le domaine temporel développé à la DER. Les premiers résultats de validation du modèle par rapport au mode fondamental de la maquette sont encourageants. Une campagne de validation complète est en cours. Enfin, les résultats du modèle sur une géométrie réelle d'assemblage combustible sont présentés, sans toutefois prendre en compte l'éventuel effet de couplage fluidélastique entre les grilles et l'écoulement, non considéré à ce stade du modèle.

EXECUTIVE SUMMARY :

In a pressurized nuclear water reactor, fuel bundles are subjected to the axial flow of primary coolant. Fluid turbulence as well as external loads cause the fuel elements to vibrate. The mean flow pressure and velocity fields depend on the motion of the fuel elements. As a result, fluid pressure and viscous forces, acting as a feedback on the structures, are motion-dependent. For axial flows, the fluid-structure coupling arising from these so-called fluidelastic forces is known to result in a significant increase in the damping. It is thus of major importance to take the fluidelastic forces into account when performing a dynamic analysis of such a system.

This paper presents an analytical model for the fluidelastic forces in bundles of slender circular cylinders subjected to an axial uniform turbulent flow. The model, developed from ideas first proposed by Païdoussis and Chen, is based on a perturbation method, assuming quasi-steady viscous fluid forces and using the slender body theory approximation. Fluidelastic pressure forces are calculated from potential theory, with hypotheses that the boundary layers are very thin and remain attached to the cylinders. The determination of the fluidelastic viscous forces amounts to considering the effect of a flow over an inclined cylinder at a very small angle of incidence : the derivative of the lift force coefficient at zero angle of incidence has to be estimated to close the model. This single parameter is set by comparison of experimental results (Tanaka & Hotta) with the predictions of the model. All of the underlying hypotheses of the model are thoroughly discussed. An extension to the original model, previously limited to circular flow channels, is proposed to analytically account for a rectangular wall. It is based on the method of images.

To further investigate the fluid-structure phenomena in arrays of cylinders subjected to an axial flow, an experimental set-up has been designed at the Research and Development Division of EDF. It consists of an array of nine Stainless Steel cylinders, either rigidly or flexibly mounted, arranged in a square pattern and confined in a square flow channel. It has been made similar to a 3 x 3 bundle of fuel elements (with respect to pitch-to-diameter ratio, reduced frequency and Reynolds number) in order to validate the model so that it could be later applied with confidence to actual fuel assemblies. The evolutions of frequency and damping ratio vs. flow velocity are inferred from the signals of strain gages processed with an original time-domain identification method. Preliminary comparisons with the model on the first mode of a single vibrating cylinder prove satisfactory. Extensive validation of the model on the EDF set-up is currently being carried on. Finally, the model is run on an actual PWR fuel assembly configuration, without considering the possible coupling between the grids and the flow which has not been incorporated in the model so far.

AN ANALYTICAL MODEL FOR THE PREDICTION OF FLUIDELASTIC FORCES IN A ROD BUNDLE SUBJECTED TO AXIAL FLOW : THEORY, EXPERIMENTAL VALIDATION AND APPLICATION TO PWR FUEL ASSEMBLIES

Frédéric Beaud
Electricité de France
R&D Division
Chatou FRANCE

NOMENCLATURE

f	Frequency (Hz).
$\vec{f}_{\tilde{p}}$	Unsteady pressure fluidelastic force (N.m^{-1}).
$\vec{f}_{\bar{p}}$	Steady pressure fluidelastic force (N.m^{-1}).
$\vec{f}_v$	Viscous fluidelastic force (N.m^{-1}).
$\vec{g}$	Acceleration of gravity (m.s^{-2}).
$p, \bar{p}, \tilde{p}$	Total, steady and unsteady pressure (Pa).
q_m	Generalized time coordinate of mode m.
s	Complex frequency (Hz).
$\vec{u}, \bar{\vec{u}}, \tilde{\vec{u}}$	Total, steady, unsteady flow velocity (m.s^{-1}).
$\bar{\vec{u}}$	Average unsteady cross-flow velocity around a cylinder (m.s^{-1}).
x_j, y_j	(x,y)-lateral deflection of cylinder j (m).
z	Axis of the bundle.
C_f	Local wall friction coefficient.
D	Drag force per unit length on a cylinder slightly inclined to the flow (N.m^{-1}).
D_h	Hydraulic diameter of the bundle (m).
H	Height of the bundle (m).
K	Number of cylinders in the bundle.
L	Lift force per unit length on a cylinder slightly inclined to the flow (N.m^{-1}).
M	Number of modes in the modal expansion.
N	Maximum order of circular harmonics.
R_0	Radius of a circular flow channel (m).
R_j	Outer radius of cylinder j (m).
Re	Reynolds number.
X_j, Y_j	(x,y)-coordinates of the center of cylinder j at rest (m).
X_0, Y_0	(x,y)-coordinates of the center of a circular flow channel (m).
$\left[F^c\right]$	Matrix of modal fluidelastic forces.
$[M], [Ma]$	Structural and added mass matrices.
$[C], [Ca]$	Structural and added damping matrices.
$[K], [Ka]$	Structural and added stiffness matrices.
ε	Wall roughness (m).
$\bar{\varepsilon}$	Dimensionless wall roughness.
$\vec{\varphi}_m^j$	Mode shape of cylinder j for mode m.
ν	Fluid kinematic viscosity (m^2.s^{-1}).
ρ	Fluid density (kg.m^{-3}).
$\bar{\bar{\tau}}$	Viscous stress tensor (Pa).
ξ	Damping ratio.

INTRODUCTION

In a pressurized nuclear water reactor, fuel bundles are subjected to the axial flow of primary coolant. Fluid turbulence as well as external loads like seismic excitation cause the fuel elements to vibrate. The motion of the fuel rods induce perturbations of the mean flow pressure and velocity fields. Fluid pressure and viscous forces on the rods, arising from these perturbations, are then motion-dependent. They are linked to the displacement, velocity and acceleration of the moving structures. In this particular configuration, the fluid-structure coupling due to these so-called fluidelastic forces is known to result in dramatic changes in the vibrational characteristics of the mechanical system, especially in a significant increase of the damping ratio. Thus, it is of major importance to take fluidelastic forces into account when performing dynamic analysis of such a mechanical system subjected to a flow of fluid.

A PWR fuel assembly can basically be represented as a bundle of slender circular cylinders supported by structural and mixing grids (figure 1). At this stage, we will concentrate on a model predicting the fluidelastic forces in such a bundle without considering the possible fluid-structure interaction between the grids and the flow. In a first section, the theoretical model is presented, emphasizing on the underlying assumptions. Then, comparisons with experimental data from the literature and first results obtained on an EDF setup are carried out. Finally, the model is run on a 17x17 bundle, simulating an actual PWR fuel assembly.

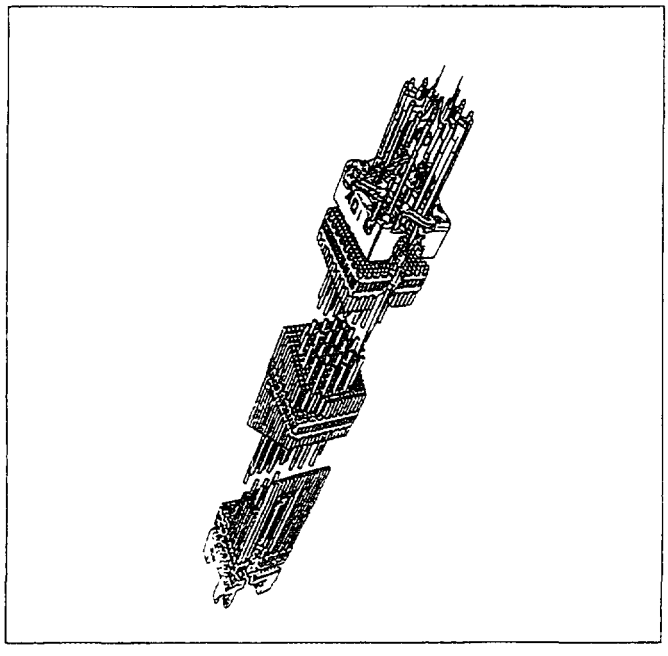

Figure 1. PWR fuel assembly.

PRESENTATION OF THE MODEL

This model is based on the work of Païdoussis and Suss (1977) from McGill University and that of Chen and Wambsganss (1972) from Argonne National Laboratory. In the 70's, they studied the dynamics of flexible cylindrical structures in bounded axial flow and developed the analytical calculation of the fluidelastic forces in this particular configuration. In this paper, we will not derive the equations of the model extensively. However, we will concentrate on the physical ideas and thoroughly list and discuss all of the underlying assumptions. Also, we will present an extension to the original model which only considered circular flow channels and show how to take a rectangular external flow boundary into account in the calculation of the fluidelastic forces. All notations are given in the nomenclature section and are described on figures 2 and 3.

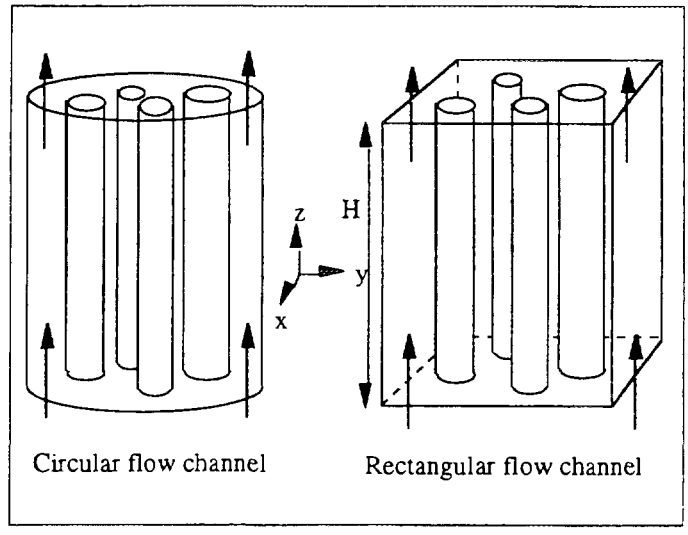

Figure 2. Circular cylinders under axial flow.

Description of the system

The system consists of a cluster of K parallel, flexible slender circular cylinders (figure 2). The cylinders are supposed to behave like Euler-Bernoulli beams and to undergo small amplitude lateral deflections. The bundle is confined in a cylindrical flow channel, either circular or rectangular, and parallel to the axis (z) of the bundle. The interval $[0, H]$ will denote the axial region of the bundle over which the fluid-structure interaction is considered. At least in this area, the geometry is supposed to be uniform. Therefore, the geometrical parameters of the system reduce to the height H of the cylinders, their diameters, the locations of their centers in the (x,y)-frame as well as the description of the flow channel cross-section (figure 3).

The motion of the bundle is given by the lateral deflections (x_j, y_j) of each cylinder j along the whole height H. Using a modal expansion, it will be written as :

$$\begin{cases} x_j(z,t) = \sum_{m=1}^{M} q_m(t)\left(\vec{\varphi}_m^j(z) \bullet \vec{x}\right) \\ y_j(z,t) = \sum_{m=1}^{M} q_m(t)\left(\vec{\varphi}_m^j(z) \bullet \vec{y}\right) \end{cases} \quad (1)$$

where M denotes the number of modes in the expansion considered to have a significant role in the motion of the system. $\vec{\varphi}_m^j$ are the corresponding modal shapes for cylinder j and mode m.

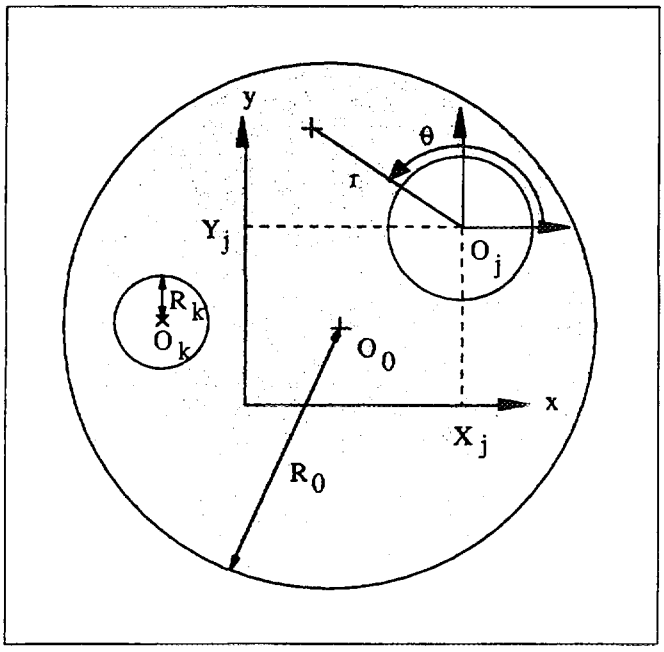

Figure 3. Description of the bundle cross-section.

Hypotheses of the model

Several hypotheses will have to be made in order to analytically solve the Navier-Stokes equations with the given boundary conditions related to the motion of the bundle. We will then be able to determine the pressure and velocity fluctuations, yielding hydrodynamic forces depending on the motion of the cylinders, i.e. the fluidelastic forces.

The Navier-Stokes equations for an incompressible flow are recalled :

$$\begin{cases} div(\rho\vec{u}) = 0 \\ \rho\left[\dfrac{\partial\vec{u}}{\partial t} + (\vec{u} \bullet \nabla)\vec{u}\right] = -\nabla p + \rho\vec{g} + div\left(\underline{\underline{\tau}}\right) \end{cases} \quad (2)$$

The fluid domain boundaries comprise the surface of the cylinders as well as the inlet and outlet of the flow. At the fluid domain entrance and exit, the fluid velocity is supposed to remain unperturbed by the motion of the bundle. The boundary conditions then reduce to a given flow velocity distribution equal to that of the steady flow. At the surface of the cylinders, the fluid velocity shall be equal to that of the structures.

As the cylinders are supposed to undergo small amplitude vibrations, we will use a perturbation method. Pressure and velocity fields are divided into steady and unsteady components as follows :

$$\begin{cases} \vec{u} = \bar{\vec{u}} + \tilde{\vec{u}} \\ p = \bar{p} + \tilde{p} \end{cases} \quad (3)$$

The unsteady fields are at least of order one compared to the steady fields. Owing to the particular geometry of the problem, the steady pressure field only depends on the axial coordinate (z) as the steady velocity field points in the z-direction. No perturbation of fluid density and viscosity will be considered here. However, fluid density and viscosity may depend on the axial coordinate z.

Four major hypotheses are made :

H1 - The Reynolds number is sufficiently high so that the boundary layers around the cylinders can be assumed to be very thin and confined at the surface of the structures. Also, because the geometry of the bundle is very smooth, the boundary layers should remain attached to the cylinders and there should not be any significant vortices in the fluid domain.

H2 - The steady flow distribution in the cross-section of the bundle will be assumed to be uniform.

H3 - The z-component of the unsteady velocity is of order two.

H4 - The fluid viscous forces on the cylinders will be determined using a quasi-steady approach.

As a consequence to hypothesis H1, the flow outside the boundary layers, i.e. in the whole fluid domain, is inviscid and irrotational. The unsteady pressure and velocity fields outside the boundary layers will then be determined using the potential flow theory. However, such an unsteady flow velocity field can only satisfy the condition on the continuity of the velocity normal component at the fluid-structure surface. Within this assumption, a tangential slip velocity thus exists at the surface of the cylinders between the fluid and the structures. It will be accounted for by using a friction law, generating a viscous fluidelastic force.

From hypothesis H2, the steady flow velocity only depends on the z-coordinate.

Hypothesis H3 is accounted for with the slender body theory which deals with the inviscid flow around a slender body, i.e. around a structure whose axial dimension is much greater than its lateral characteristic lengths and to which the oncoming flow has an angle of incidence of order one. The slender body theory, presented in Hinch (1991), assumes that the flow is actually

extending to infinity, which is obviously not satisfied in our problem. However, one is also quite far from a configuration where the radial component of the unsteady flow velocity is generally neglected, like in the case of a narrow annular flow (Perotin, 1994).
The quasi-steady approach (hypothesis H4), as well as the slender body approximation, assumes that the order of magnitude of the bundle lateral velocity is of order one compared to the axial flow velocity.

Constitutive equations of the model

The steady part of the Navier-Stokes equations yields the mean flow velocity and pressure axial distributions. The steady pressure axial gradient is :

$$\frac{d\bar{p}}{dz} = -\rho\,\bar{u}\,\frac{d\bar{u}}{dz} - 2\,\rho\,\frac{C_f}{D_h}\,|\bar{u}|\,\bar{u} + \rho\,\vec{g}\bullet\vec{z} \tag{4}$$

The local wall friction coefficient C_f, determined from equivalent pipe pressure loss correlations (Idel'cik, 1969), depends on the Reynolds number Re based on the steady flow velocity and on the roughness of the wall $\bar{\varepsilon}$ made dimensionless with the hydraulic diameter of the bundle. The correlations used in the model are given in appendix A.
As a consequence to hypotheses H1 and H3, the unsteady flow velocity will be written as the gradient of an unknown potential field :

$$\tilde{\vec{u}} = \nabla_{x,y}\tilde{\phi} \tag{5}$$

The boundary conditions on the potential field in the transformed coordinate system where the bundle is at rest can be shown to be (Lighthill, 1960b) :

$$\begin{cases} \dfrac{\partial\tilde{\phi}}{\partial x}(x,y,z,t) = \left[\dfrac{\partial}{\partial t} + \bar{u}(z)\dfrac{\partial}{\partial z}\right] x_j(z,t) = \dfrac{Dx_j}{Dt}(z,t) \\ \dfrac{\partial\tilde{\phi}}{\partial y}(x,y,z,t) = \left[\dfrac{\partial}{\partial t} + \bar{u}(z)\dfrac{\partial}{\partial z}\right] y_j(z,t) = \dfrac{Dy_j}{Dt}(z,t) \end{cases} \tag{6}$$

To analytically determine the unsteady flow velocity, we will use a singularity method (Kundu, 1990). In any bundle cross-section, each cylinder is replaced by a linear series of the following circular harmonics written in the coordinate system centered on its axis (Batchelor, 1967) :

$$r^{-n}\cos(n\theta),\ r^{-n}\sin(n\theta) \tag{7a}$$

To represent the influence of a cylindrical circular flow channel, an additional set of circular harmonics centered on the channel axis is used, since we are now dealing with an inner flow :

$$r^{n}\cos(n\theta),\ r^{n}\sin(n\theta) \tag{7b}$$

These harmonics are very useful to deal with circular structures as the use of polar coordinates obviously makes the derivation of the boundary conditions straightforward. However, when dealing with a non-circular flow channel, which may occur quite often, it becomes very difficult to work out the equations analytically if using this kind of elementary solutions of the Laplace equation. We will take advantage of the method of images, commonly used in aeronautics : In the particular problem of the influence of a wall on the potential flow around an airfoil, it is equivalent to consider the flow around the airfoil itself and its symmetry with respect to the wall (figure 4). As a matter of fact, the flow around these two structures is necessarily symmetric and then automatically satisfies the continuity of the velocity normal component at the wall. In the case of a rectangular channel surrounding the structures, it is slightly more complicated but the basic idea remains the same and amounts to reflecting the cylinders with respect to each of the four walls. One has to be careful how these virtual cylinders are constructed so as to eventually obtain a pattern of streamlines symmetrical with respect to the walls. This method is detailed in appendix B.
The unsteady flow field can be written as follows for a circular channel,

$$\begin{aligned} \tilde{\phi} = &\sum_{n=1}^{N}\left[A_n\,r_0^n\cos(n\theta_0) + B_n\,r_0^n\sin(n\theta_0)\right] \\ &+ \sum_{j=1}^{K}\sum_{n=1}^{N}\left[C_{nj}\,r_j^{-n}\cos(n\theta_j) + D_{nj}\,r_j^{-n}\sin(n\theta_j)\right] \end{aligned} \tag{8a}$$

and for a rectangular channel,

$$\tilde{\phi} = \sum_{j=1}^{K+K'}\sum_{n=1}^{N}\left[C_{nj}\,r_j^{-n}\cos(n\theta_j) + D_{nj}\,r_j^{-n}\sin(n\theta_j)\right] \tag{8b}$$

where K' virtual cylinders have been constructed by reflection and circular harmonics up to order N are considered.
Each term of these series must depend on the motion of the whole bundle. The unknown coefficients A_n, B_n, C_{nj}, D_{nj} are determined using the boundary conditions and can be expressed as follows :

$$\begin{cases} A_n(z,t) = R_0^{1-n}\displaystyle\sum_{k=1}^{K}\left[\alpha_{nk}\frac{Dx_k}{Dt}(z,t) + a_{nk}\frac{Dy_k}{Dt}(z,t)\right] \\ B_n(z,t) = R_0^{1-n}\displaystyle\sum_{k=1}^{K}\left[\beta_{nk}\frac{Dx_k}{Dt}(z,t) + b_{nk}\frac{Dy_k}{Dt}(z,t)\right] \\ C_{nj}(z,t) = R_j^{n+1}\displaystyle\sum_{k=1}^{K}\left[\gamma_{njk}\frac{Dx_k}{Dt}(z,t) + c_{njk}\frac{Dy_k}{Dt}(z,t)\right] \\ D_{nj}(z,t) = R_j^{n+1}\displaystyle\sum_{k=1}^{K}\left[\delta_{njk}\frac{Dx_k}{Dt}(z,t) + d_{njk}\frac{Dy_k}{Dt}(z,t)\right] \end{cases} \tag{9}$$

After lengthy manipulations, the unknown coefficients $\alpha_{nk}, a_{nk}, \beta_{nk}, b_{nk}, \gamma_{njk}, c_{njk}, \delta_{njk}, d_{njk}$ are derived by using the boundary conditions. The results of the calculations are given by Païdoussis and Suss (1977) in the case of a circular flow channel.

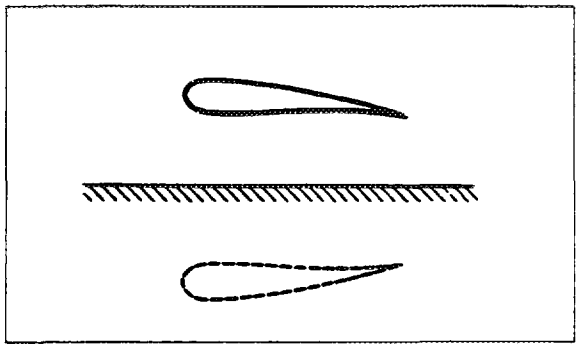

Figure 4. Method of images applied to an airfoil in the vicinity of a wall.

Expression of fluidelastic forces

Fluidelastic forces, i.e. the fluid forces arising from the motion of the cylinders and acting on the bundle, can be divided into three categories :

- the fluid forces due to the unsteady pressure field,
- the fluid forces due to the steady pressure field acting on the deformed structures,
- the viscous fluid forces in the boundary layer due to the steady and unsteady flow velocity fields.

We will subsequently only consider the (x,y)-components of these forces per unit length which affect the lateral motion of the cylinders.

Unsteady pressure fluidelastic forces. From hypothesis H1, the flow outside the boundary layers is inviscid and irrotational. Then the relationship between the unsteady pressure and potential field is :

$$\tilde{p} = -\rho \left[\frac{\partial \tilde{\phi}}{\partial t} + \bar{u} \frac{\partial \tilde{\phi}}{\partial z} \right] = -\rho \frac{D\tilde{\phi}}{Dt} \tag{10}$$

This field can be analytically estimated at the surface of the cylinders. One has to outline that the boundary layer, which was nevertheless assumed to be very thin, lies between the fluid domain region close to the cylinders and the structures themselves. In order to evaluate the pressure force on the cylinders resulting from this unsteady field, an additional assumption must be made : The normal pressure gradient across the boundary layer is supposed to be negligible. Then, integrating the unsteady pressure field around cylinder ℓ yields the following (x,y)-force :

$$\tilde{f}_{\tilde{p}}^{\ell} = -\rho \pi R_\ell^2 \sum_{k=1}^{K} \left\{ \begin{pmatrix} \varepsilon_{\ell k} \\ \zeta_{\ell k} \end{pmatrix} \frac{D^2 x_k}{Dt^2} + \begin{pmatrix} e_{\ell k} \\ f_{\ell k} \end{pmatrix} \frac{D^2 y_k}{Dt^2} \right\} \tag{11}$$

The coefficients $\varepsilon_{\ell k}, e_{\ell k}, \zeta_{\ell k}, f_{\ell k}$ are related to $\alpha_{nk}, a_{nk}, \beta_{nk}, b_{nk}, \gamma_{njk}, c_{njk}, \delta_{njk}, d_{njk}$ (Païdoussis and Suss, 1977).

Steady pressure fluidelastic forces. It can be easily shown that the integration of the steady pressure field on the deformed surface of cylinder ℓ leads to the following fluid force per unit length :

$$\bar{f}_{\bar{p}}^{\ell} = \pi R_\ell^2 \frac{\partial}{\partial z} \left[\bar{p}(z) \frac{\partial}{\partial z} \begin{pmatrix} x_\ell(z,t) \\ y_\ell(z,t) \end{pmatrix} \right] \tag{12}$$

Viscous fluidelastic forces. As explained above, there is a difference in the tangential component of the velocity between the structures and the fluid domain across the boundary layer separating them. Indeed, the calculated fluid velocity field only considered the condition of continuity of the velocity normal component. This difference produces viscous stresses in the boundary layers which remain attached to the structures. Using the appropriate coordinate transformation which would bring the bundle back into its position at rest (Lighthill, 1960b), it can be shown that the cross-section of each cylinder is actually subjected to a flow at nominal velocity and with pitch angles i_x and i_y relative to its axis of order one in the (x,z) and (y,z)-frame, respectively. These angles not only include the inclination of the cylinder but also the apparent velocity due to its lateral motion as well as the averaged unsteady velocity around the cross-section (figure 5). The averaged unsteady velocity components around cylinder ℓ can be expressed in terms of the characteristics of the bundle motion as :

$$\begin{aligned} \bar{\tilde{u}}_x^{\ell} &= \frac{1}{2\pi} \int_0^{2\pi} \tilde{u}_x \, d\theta_\ell = \sum_{k=1}^{K} \left[\nu_{\ell k} \frac{Dx_k}{Dt} + \eta_{\ell k} \frac{Dy_k}{Dt} \right] \\ \bar{\tilde{u}}_y^{\ell} &= \frac{1}{2\pi} \int_0^{2\pi} \tilde{u}_y \, d\theta_\ell = \sum_{k=1}^{K} \left[\bar{\nu}_{\ell k} \frac{Dx_k}{Dt} + \bar{\eta}_{\ell k} \frac{Dy_k}{Dt} \right] \end{aligned} \tag{13}$$

In order to evaluate the fluid forces on a cylinder at time t, we will assume that they are equal to the forces on an infinitely long cylinder of the same inclination after a sufficient amount of time to reach asymptotic flow conditions. This is the quasi-steady hypothesis formulated above (H4). In the configuration of figure 5, the fluid forces per unit length are divided into a drag component D, inline with the flow, and a lift component L, perpendicular to the flow.

As the angles of incidence $i = i_x, i_y$ are of order one, an expansion around zero may be carried out and yields :

$$\begin{cases} D = D_0 + \left(\dfrac{\partial D}{\partial i}\right)_{i=0} \times i = \rho\, R_\ell\, \pi\, C_f\, \bar{u}^2 + \left(\dfrac{\partial D}{\partial i}\right)_{i=0} \times i \\ L = L_0 + \left(\dfrac{\partial L}{\partial i}\right)_{i=0} \times i = \rho\, R_\ell\, C_p\, \bar{u}^2\, i \end{cases} \quad (14)$$

For reasons of symmetry, the lift L_0 must be zero. The drag D_0 at zero angle of incidence can be determined from the pressure drop correlations in piping systems, in terms of the local wall friction coefficient C_f (Idel'cik, 1969). At this point, both the derivatives of the lift and drag coefficients at zero angle of incidence are unknown. However, the drag derivative will drop out when considering the lateral viscous fluidelastic forces which are :

$$\begin{cases} \left(\bar{f}_v^\ell\right)_x \approx \rho\, R_\ell\, \bar{u} \left[C_p \left(\tilde{u}_x - \dfrac{D x_\ell}{Dt} \right) + \pi\, C_f \left(\tilde{u}_x - \dfrac{\partial x_\ell}{\partial t} \right) \right] \\ \left(\bar{f}_v^\ell\right)_y \approx \rho\, R_\ell\, \bar{u} \left[C_p \left(\tilde{u}_y - \dfrac{D y_\ell}{Dt} \right) + \pi\, C_f \left(\tilde{u}_y - \dfrac{\partial y_\ell}{\partial t} \right) \right] \end{cases} \quad (15)$$

Only the lift coefficient derivative remains unknown. To the author's knowledge, no fundamental study can be found in the literature about lift forces around cylinders for very small angles of attack. Also, it is believed that the physics of the flow in the vicinity of a zero angle of incidence widely differs from that at higher pitch angles and that the data about flows around circular cylinders for quite large angles of incidence (Taylor, 1952, Hoerner, 1965) can not be properly extrapolated. At this stage, a single value of $C_p = 0.08$ will subsequently be used and shown to fit experimental data in a wide range of cases. It is important to outline that neglecting this lift force would not lead to proper results with regard to the experimental observations.

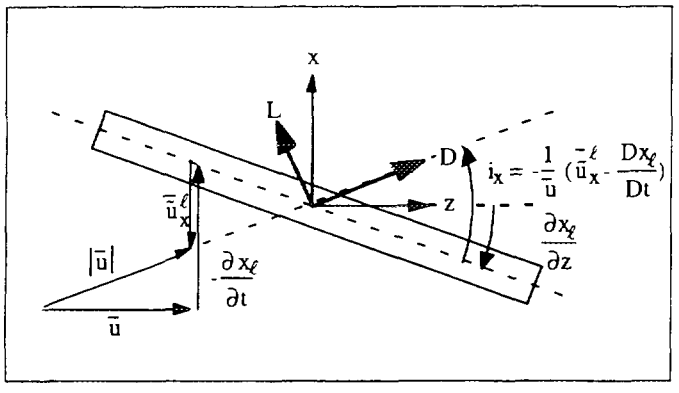

Figure 5. Flow around the cross-section of a flexible cylinder.

Numerical solution to the model

As explained above, we will seek a solution to this model based on a modal approach. Without the coupling with the axial flow, the equations of motion of the bundle in terms of the generalized coordinates $\{q(s)\}$ in the Laplace domain are :

$$\left([M]\, s^2 + [C]\, s + [K]\right) \{q(s)\} = \{0\} \quad (16)$$

$[M]$, $[C]$ and $[K]$are the structural mass, damping and stiffness matrices, respectively. Substituting equation (1) into equations (11), (12) and (15), multiplying by the mode shape $\bar{\varphi}_i$ and integrating over the whole height of the bundle, one obtains the following generalized fluidelastic force for mode i :

$$\begin{aligned} F_i^c(s) &= \sum_{\ell=1}^{K} \left(\int_0^H \left(\bar{f}_p^\ell(z,s) + \bar{f}_{\bar{p}}^\ell(z,s) + \bar{f}_v^\ell(z,s) \right)_j \bullet \bar{\varphi}_i^\ell(z) \right) \\ &= \sum_{j=1}^{M} F_{ij}^c(s)\, q_j(s) \end{aligned} \quad (17)$$

From equations (11), (12) and (15), the matrix $\left[F^c(s)\right]$ can be expressed as a second order polynomial function of the complex frequency s as follows :

$$\left[F^c(s)\right] = -[Ma]\, s^2 - [Ca]\, s - [Ka] \quad (18)$$

Owing to the particular configuration of the present problem, the added damping and stiffness matrices, $[Ca]$ and $[Ka]$ respectively, are independent of the complex frequency s. Since the model takes a possible coupling between modes into account, all of the three matrices $[Ma]$, $[Ca]$ and $[Ka]$ are full. Only the added mass matrix $[Ma]$ is symmetric.

The equations of motion of the coupled fluid-structure system are :

$$\left([Mc]\, s^2 + [Cc]\, s + [Kc]\right) \{q(s)\} = \{0\} \quad (19)$$

with :

$$[Mc] = [M] + [Ma],\ [Cc] = [C] + [Ca],\ [Kc] = [K] + [Ka] \quad (20)$$

Equation (19) can be re-written in the form :

$$\begin{bmatrix} 0 & [Id] \\ -[Mc]^{-1}[Kc] & -[Mc]^{-1}[Cc] \end{bmatrix} \begin{Bmatrix} q(s) \\ s\, q(s) \end{Bmatrix} = s \begin{Bmatrix} q(s) \\ s\, q(s) \end{Bmatrix} \quad (21)$$

The eigenvalues and eigenvectors of equation (21) are obtained by standard methods. Complex eigenvalues s are classically written as :

$$s = -2\pi f \xi \pm 2\pi f \sqrt{1 - \xi^2} \quad (22)$$

where f and ξ are the frequency and damping ratio of the coupled fluid-structure system, respectively. The eigenvectors are also complex. In order to derive the corresponding mode shapes for physical interpretation, one should first estimate equivalent real components from the eigenvectors. This is done by calculating the complex coefficient of proportionality which minimizes the imaginary part of the eigenvectors.

RESULTS OF THE MODEL AND COMPARISONS WITH EXPERIMENTAL DATA

The model presented above will be applied to determine the evolutions of modal frequencies and damping ratios of bundles of circular cylinders subjected to axial flow. The initial estimates of the dynamical characteristics of the system in air are of major importance. Indeed, the fluidelastic forces largely depend on the mode shapes of the cylinders. Also, the frequency in air and structural modal mass arise in the estimation of the damping ratio of the fluid-structure system from the physical forces determined by the model. In the following computations, the mechanical systems are first modeled using the EDF computer code of mechanics, *Code_Aster*. Their modal characteristics without fluid coupling are thus calculated.

Available data from the literature

Two cases from the literature will be tested first (Tanaka et al., 1988, Hotta et al., 1990). Case A represents a single flexible PVC tube confined in a circular flow channel. Case B represents a bundle of nine flexible Aluminium tubes maintained by piano wires at their mid-span, arranged in a 3x3 square array and confined in a rectangular flow channel. In both cases, each flexible cylinder is maintained at their lower and upper ends by a short thin tube, thus simulating approximate pinned-pinned support conditions. The systems are subjected to a flow of water at room temperature. In case A, two different pre-load conditions of the flexible cylinders are tested.
The frequency and damping ratio of the first mode of the system are reported, except for the evolution of frequency in case A. They compare satisfactorily with the results of the model (figures 6 and 7).

EDF experimental set-up

In order to further validate this theoretical model, an experimental apparatus was set up at the Research and Development Division of EDF. Since we aim at predicting the influence of the axial flow of primary coolant on PWR fuel assemblies, special care was taken to design the mock-up as closely as possible to the actual in-core operating conditions, in terms of dimensionless numbers. Reduced frequencies of the first two modes and Reynolds number are made similar to those of typical fuel assemblies. The bundle is made of a 3x3 array of cylinders with a pitch-to-diameter ratio of 1.33 identical to the arrangement of fuel rods.

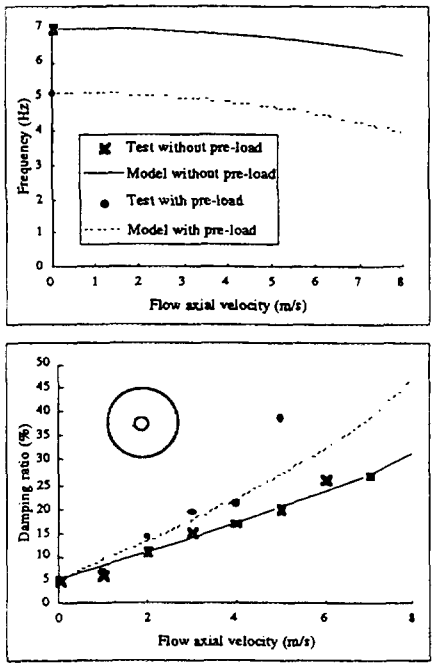

Figure 6. Evolutions of frequency and damping ratio vs. flow velocity in case A (Tanaka et al., 1988).

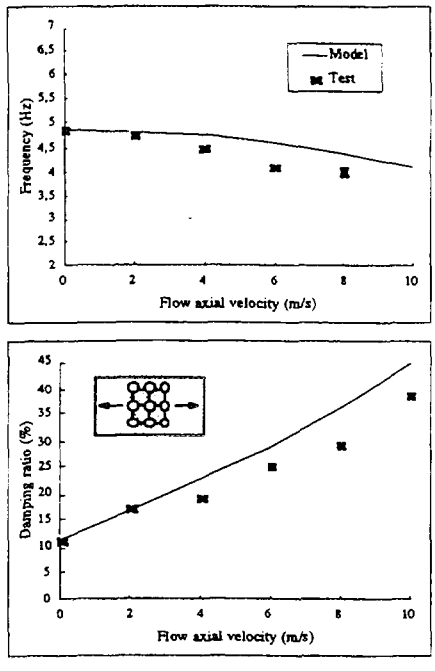

Figure 7. Evolutions of frequency and damping ratio vs. flow velocity in case B (Hotta et al., 1990).

The 3x3 bundle is confined in a 129x129 mm^2 flow channel and subjected to a flow of water at room temperature. Each cylinder is actually made of two separate tubes : the inner tube, with inside and outside diameters of 6 and 8 mm respectively, is clamped at its upper end and maintained by a Plexiglas washer at its lower end. The 1 m long outer tube, with inside and outside diameters of 20 and 30 mm respectively, is connected to the flexible inner tube at about 6/10th of its span. It is very stiff and can be assumed to undergo only rigid body motions. Only the outer tube, about three times as large in diameter as a fuel rod, is subjected to the flow. The inner tube is equipped with four strain gages. The signals from the gages are post-processed using an original time-domain modal identification method developed at EDF (Granger, 1990). Frequency and damping of the first two modes are measured in air, in quiescent water and under flow. The first and second modes result in translational and rotational motions of the outer tube, respectively.

Preliminary results are presented here for a single flexible cylinder located at the center of the test section. The evolutions of frequency and damping ratio on the first mode compare satisfactorily with the predictions of the model (figure 8).

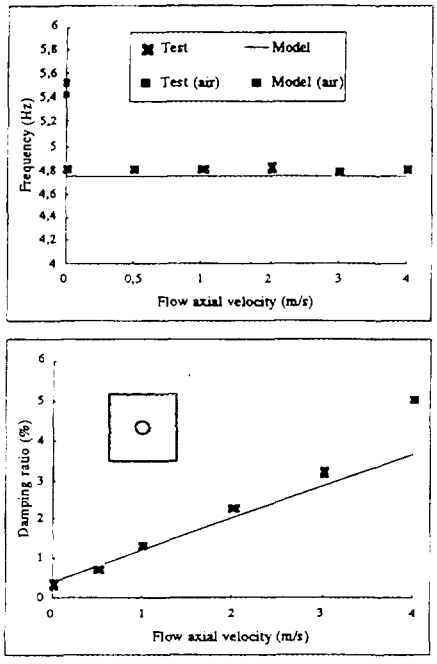

Figure 8. Comparisons of calculated and measured values of frequency and damping ratio vs. flow velocity on the EDF set-up.

Simulation of an actual PWR fuel assembly

Finally, the influence of the primary coolant flow on the vibrational characteristics of a 900MW PWR fuel assembly under flow was studied. An equivalent two-beam model was used to simulate the dynamics of the assembly with the *Code_Aster* Finite Element computer code. The first beam represents the fuel rods and the second one accounts for the guide thimble tubes. The effects of the springs and arches of the grids are simulated using translational and rotational spring elements (Jacquart, 1995).

Again, only the first mode of the system is considered here. Neglecting the structural damping, the evolutions of the vibrational characteristics, i.e. frequency and damping ratio, of the coupled fluid-structure system are reported on figure 9. Damping is only to be attributed to fluid effect. A 215.86x215.86 mm^2 flow channel is considered in order to simulate the influence of the surrounding assemblies. The flow velocities of interest range from 4.0 to 5.0 $m.s^{-1}$, the nominal flow velocity being about 4.4 $m.s^{-1}$ in a 900MW nuclear reactor. It is shown to increase from 10% to about 14% with flow velocity whereas frequency slightly decreases with flow rate because of added mass from quiescent water and negative added stiffness from the flow. The water density and viscosity used in these calculations corresponds to a core temperature of 280°C. It is important to emphasize that the model does not include the possible coupling effect between the flow and the grids. It is reported to be significant (Hotta et al., 1990) and will soon be investigated at EDF.

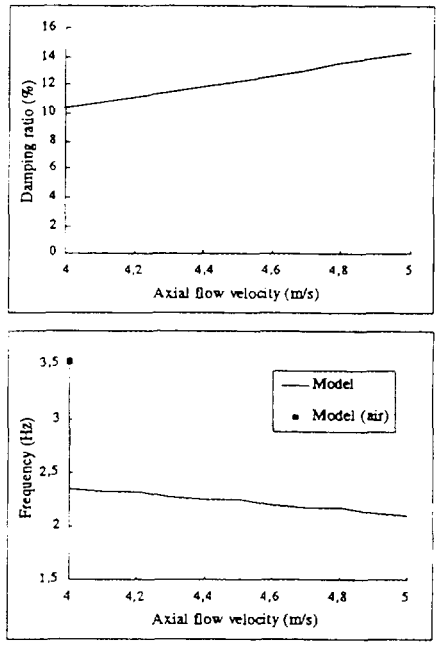

Figure 9. Evolutions of frequency and damping for the first mode of a 900MW fuel assembly.

CONCLUSIONS

A model predicting the fluidelastic forces in a bundle of circular cylinders subjected to axial flow was presented in this paper. Whereas previously published models were limited to circular flow channel, the present one allows to take a rectangular flow external boundary into account. For that purpose, an original approach was derived from the standard method of images.

This model will eventually be used to predict the fluid-structure coupling between the flow of primary coolant and the fuel assemblies in PWR nuclear reactors. It is indeed of major importance since the flow is shown to induce quite high damping and could therefore mitigate the incidence of an external load like a seismic excitation on the dynamics of the assemblies.

The proposed model has been validated on two cases from the literature but still needs further comparisons with the experiments being currently carried out on the EDF set-up. The flow has been shown to induce an approximate 12% damping on a PWR fuel assembly, at nominal reactor conditions. The possible grid effect on the fluid-structure coupling has been neglected so far but will soon be investigated at EDF.

ACKNOWLEDGMENTS

The author is very grateful to the engineers at the Research and Development Division of EDF who participated in the modeling of the PWR fuel assembly and performed the calculations with the *Code_Aster* computer code. Special thanks are addressed to G. Jacquart and Fe. Waeckel.

REFERENCES

Batchelor, G.K., 1967, "An Introduction to Fluid Dynamics", Cambridge University Press, pp. 124-130.

Chen, S.S., and Wambsganss, M.W., 1972, "Parallel-Flow-Induced Vibration of Fuel Rods", *Nuclear Engineering and Design*, Vol. 18, pp. 253-278.

Granger, S., 1990, "A New Signal Processing Method for Investigating Fluidelastic Phenomena", *Journal of Fluids and Structures*, Vol. 4, pp. 73-97.

Hinch, E.J., 1991, "Perturbation Methods", Cambridge Texts in Applied Mathematics, Cambridge University Press, Cambridge, pp. 42-45, 90-92.

Hoerner, S.F., 1965, "Résistance à l'avancement dans les fluides", Gauthier-Villars, ed., Paris, p. 48.

Hotta, A., Niibori, H., Tanaka, M., and Fujita, K., 1990, "Parametric Study on Parallel Flow-Induced Damping of PWR Fuel Assembly", *Proceedings, 1990 ASME Pressure Vessels and Piping Conference*, Nashville, TN, Vol. 191, pp. 89-98.

Idel'cik, I.E., 1969, "Memento des Pertes de Charge", Collection de la Direction des Etudes et Recherches d'Electricité de France, Eyrolles, ed., pp. 55-80.

Jacquart, G., 1995, "Computing PWR fuel assemblies behaviour under seismic solicitations", *Proceedings, 13th SMIRT International Conference on Structural Mechanics in Reactor Technology*, Porto-Alegre, Brasil.

Kundu, P.K., 1990, "Fluid Mechanics", Academic Press, Inc., pp. 162-163.

Lighthill, M.J., 1960a, "Mathematics and Aeronautics", *Journal of the Royal Aeronautical Society*, Vol. 64, pp. 375-394.

Lighthill, M.J., 1960b, "Note on the swimming of slender fish", *Journal of Fluid Mechanics*, Vol. 9, pp. 305-317.

Païdoussis, M.P., and Suss, S., 1977, "Stability of a Cluster of Flexible Cylinders in Bounded Axial Flow", *Journal of Applied Mechanics*, Vol. 44, pp. 401-408.

Perotin, L., 1994, "Fluid-Structure Coupling between a Vibrating Cylinder and a Narrow Annular Flow", *Nuclear Engineering and Design*, Vol. 149, pp. 279-289.

Sears, W.R., 1960, "Small Perturbation Theory", *Princeton Aeronautical Paperbacks*, Number 4, Princeton University Press, Princeton, NJ, pp. 18-20, 38-41.

Tanaka, M., Fujita, K., Hotta, A., and Kono, N., 1988, "Parallel Flow-Induced Damping of PWR Fuel Assembly", *Proceedings, 1988 ASME Pressure Vessels and Piping Conference*, Pittsburgh, PA, Vol. 133, pp. 121-125.

Taylor, G.I., 1952, "Analysis of the swimming of long and narrow animals", *Proceedings of the Royal Society of London*, Vol. 214, Series A, pp. 158-183.

APPENDIX A

CORRELATIONS FOR WALL FRICTION COEFFICIENT

The following correlations are taken from Idel'cik (1969).

The Reynolds number Re is based on the hydraulic diameter and on the mean flow axial component :

$$Re = \frac{D_h |\overline{u}|}{\nu} \tag{23}$$

Two critical Reynolds numbers are defined. The critical Reynolds number from hydraulically smooth turbulent flow to transitional flow is set equal to :

$$Re_1 = \frac{23}{\bar{\varepsilon}} \tag{24a}$$

The critical Reynolds number from transitional flow to fully turbulent flow is defined as :

$$Re_2 = \frac{560}{\bar{\varepsilon}} \tag{24b}$$

The wall roughness is made dimensionless with the hydraulic diameter of the bundle :

$$\bar{\varepsilon} = \frac{\varepsilon}{D_h} \tag{25}$$

The local wall friction coefficient C_f is then calculated from the diagram below :

$Re < 2000 \rightarrow C_f = 16\, Re^{-1}$ (26a)

no ↓

$Re < 4000 \rightarrow C_f = 1.2 \times 10^{-4}\, Re^{0.55}$ (26b)

no ↓

$Re < Re_1 \rightarrow C_f = 0.25 \left(1.8\, log_{10}(Re) - 1.64\right)^{-2}$ (26c)

no ↓

$\left.\begin{matrix} Re > Re_1 \\ Re < Re_2 \end{matrix}\right\} \rightarrow C_f = 0.025 \left(1.46\, \bar{\varepsilon} + 100\, Re^{-1}\right)^{0.25}$ (26d)

no ↓

$Re > Re_2 \rightarrow C_f = 0.25 \left(2\, log_{10}\left(3.7\, \bar{\varepsilon}^{-1}\right)\right)^{-2}$ (26e)

APPENDIX B

METHOD OF IMAGES FOR A RECTANGULAR FLOW CHANNEL

To illustrate, let us consider the two-dimensional motion of a single cylinder in a rectangular flow channel. In order to analytically express the unsteady flow velocity field due to the motion of the cylinder, we will consider a series of circular harmonics of the form (7a) to represent the influence of the cylinder on the flow. The coefficients of the series will be later determined using the condition of continuity of the velocity normal component. This latter condition must also be satisfied at the wall of the flow channel. Its application when dealing with circular boundaries is rendered fairly easy by the use of polar coordinates (Païdoussis and Suss, 1977). However, it would be far more complicated with a straight wall. Therefore, we will extend the classical method of images to a rectangular channel. This method allows to omit the wall but introduces a number of singularities derived from the original circular harmonics.

A first virtual cylinder is introduced as image of the original one with respect to side one of the channel (step 1). Starting from this virtual cylinder, new images with respect to the different sides of the channel are successively introduced as depicted on figure 10. A first turn around the flow external boundary is created from step 2 to step 8. Another turn is constructed the same way from step 9 on. If repeating the procedure to infinity, one obtains a geometrical pattern symmetrical with respect to each wall of the rectangular channel. Circular harmonics derived from those representing the original cylinder are placed at the center of each virtual cylinder. Going from cylinder j to cylinder $j+1$, the basic harmonics given by equation (7a) are transformed in the following way :

$$\begin{cases} r^{-n}\cos(n\theta) \rightarrow r^{-n}\cos[n(\theta-2\alpha)] \\ r^{-n}\sin(n\theta) \rightarrow -r^{-n}\sin[n(\theta-2\alpha)] \end{cases} \tag{27}$$

where α is the angle of the wall with respect to the x-axis.

With this transformation, the streamlines generated by all the singularities are symmetrical with respect to each of the channel sides. The continuity condition of the velocity normal component is then automatically satisfied. For computational purposes, one is limited to a finite number of turns around the original cell. The influence of the singularities decreases with the distance to the original cell. Therefore, this process converges quite quickly and can be practically truncated after 10 turns. The results of the method and the rate of convergence were tested by comparison of added mass terms with a numerical method. It proved very efficient.

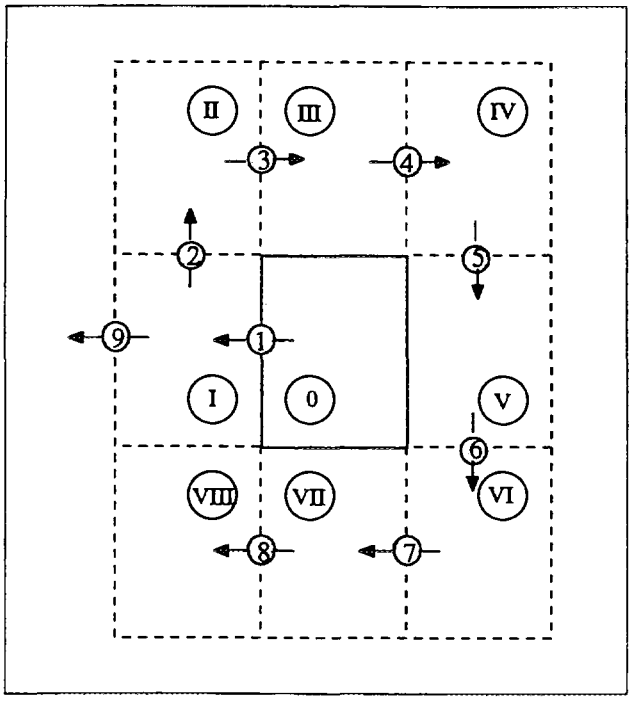

Figure 10. Construction of virtual cylinders.